

Bose-Einstein condensates in 1D optical lattices: compressibility, Bloch bands and elementary excitations

¹M. Krämer, ^{1,2}C. Menotti, ^{1,3}L. Pitaevskii and ¹S. Stringari

¹ *Dipartimento di Fisica, Università di Trento and BEC-INFM, I-38050 Povo, Italy*

² *Dipartimento di Matematica e Fisica, Università Cattolica del Sacro Cuore, I-25121 Brescia, Italy*

³ *Kapitza Institute for Physical Problems, 117334 Moscow, Russia*

(October 21, 2018)

We discuss the Bloch-state solutions of the stationary Gross-Pitaevskii equation and of the Bogoliubov equations for a Bose-Einstein condensate in the presence of a one-dimensional optical lattice. The results for the compressibility, effective mass and velocity of sound are analysed as a function of the lattice depth and of the strength of the two-body interaction. The band structure of the spectrum of elementary excitations is compared with the one exhibited by the stationary solutions (“Bloch bands”). Moreover, the numerical calculations are compared with the analytic predictions of the tight binding approximation. We also discuss the role of quantum fluctuations and show that the condensate exhibits 3D, 2D or 1D features depending on the lattice depth and on the number of particles occupying each potential well. We finally show how, using a local density approximation, our results can be applied to study the behaviour of the gas in the presence of harmonic trapping.

I. INTRODUCTION

Cold atoms in optical lattices exhibit phenomena typical of solid state physics like the formation of energy bands, Bloch oscillations, and Josephson effects. Many of these phenomena have been already the object of experimental and theoretical investigation in Bose-Einstein condensates. For deep potential wells further important effects take place like the transition from the superfluid to the Mott insulator phase [1,2].

The purpose of this paper is to study some structural properties of interacting Bose-Einstein condensed dilute gases at $T = 0$ in the presence of 1D periodic potentials generated by laser fields (1D optical lattices). Unless the confinement in the radial direction is very tight, the transition to the insulator phase in 1D optical lattices is expected to take place only for extremely deep potential wells. There is consequently a large range of potential depths where the gas can be described as a fully coherent system, in the framework of the mean field Gross-Pitaevskii approach to the order parameter.

We will explicitly discuss the change in the behaviour of the system as a function of the optical potential depth, ranging from the uniform gas (absence of optical lattice) to the opposite regime of deep wells separated by high barriers (tight binding limit). Special emphasis will be given to the role of two-body interactions, whose effects

will be addressed by varying the average density n .

An important feature produced by the periodic potential is the occurrence of a typical band structure in the energy spectra. In this paper we will discuss different manifestations of such a band structure, including:

- the energy per particle $\varepsilon_j(k)$ of stationary Bloch-wave configurations consisting in the motion of the whole condensate and carrying a current constant in time and uniform in space (“Bloch bands”). This energy is naturally parametrized as a function of the quasimomentum k which, together with the band index j ($j = 1, 2, \dots$), is the proper quantum number of these states;

- the chemical potential

$$\mu_j(k) = \frac{\partial[n\varepsilon_j(k)]}{\partial n}, \quad (1)$$

of the same stationary configurations, where n is the average density of the sample. The chemical potential plays a crucial role in the determination of the equation of state and emerges as a natural output of the solution of the Gross-Pitaevskii equation (see Eq.(10) below);

- the spectrum $\hbar\omega_j(q)$ of the elementary excitations (“Bogoliubov bands”) carrying quasi-momentum q . The elementary excitations are small perturbations of the system and in general can be calculated with respect to each stationary configuration of quasimomentum k . In this paper we will limit the discussion to the elementary excitations built on top of the groundstate configuration ($k = 0$). They can be determined by solving the linearized Gross-Pitaevskii equations (see Eqs.(25,26)).

The three band spectra ε_j , μ_j and $\hbar\omega_j$ represent different physical quantities and have the same dependence on quasimomentum only in the absence of two body interactions. Due to the periodicity of the problem the quasi-momentum can be restricted to the first Brillouin zone. Still it is often convenient to consider all values of quasi-momentum to emphasize the periodicity of the energy spectra in quasi-momentum space.

In Sect.II, we discuss the equation of state and the Bloch bands, assuming uniform confinement in the radial direction. Special emphasis is given to the behaviour of the compressibility and the effective mass. The compressibility κ is defined by the thermodynamic relation

$$\kappa^{-1} = n \frac{\partial\mu}{\partial n}, \quad (2)$$

where μ is the chemical potential relative to the groundstate solution of the Gross-Pitaevskii equation ($\mu \equiv$

$\mu_{j=1}(k=0)$). For systems interacting with repulsive forces, the optical trapping reduces the compressibility of the system since the effect of repulsion is enhanced by the squeezing of the condensate wavefunction in each well. The effective mass is defined through the curvature of the lowest ($j=1$) energy band

$$\frac{1}{m^*(k)} = \frac{\partial^2 \varepsilon}{\partial k^2}. \quad (3)$$

Here and in the following, we omit the band index j when we refer to the lowest band ($j=1$). The current flowing along the direction of the optical lattice, is fixed by the relation

$$I(k) = n \frac{\partial \varepsilon}{\partial k}, \quad (4)$$

and in the long wavelength limit $k \rightarrow 0$, one finds $I \rightarrow nk/m^*$, where we have used the notation $m^* \equiv m^*(k=0)$. Equivalently, one has

$$\varepsilon(k) \xrightarrow{k \rightarrow 0} \varepsilon(k=0) + \frac{k^2}{2m^*}. \quad (5)$$

For small intensities of the laser field the effective mass m^* approaches the bare value m . Instead, for large intensities the effective mass is inversely proportional to the tunneling rate through the barrier separating neighbouring potential wells and is strongly enhanced with respect to the bare value.

Based on the knowledge of the compressibility and of the effective mass, one can calculate the sound velocity according to the thermodynamic relation

$$c = \frac{1}{\sqrt{\kappa m^*}}. \quad (6)$$

This quantity fixes the slope of the lowest Bogoliubov band at low quasi momenta.

In Sect.III, we discuss the behaviour of the elementary excitations. The excitation spectrum (Bogoliubov spectrum) is obtained from the solution of the linearized time-dependent Gross-Pitaevskii equation and develops energy bands $\hbar\omega_j(q)$ periodic in quasi-momentum space. From the same solutions one can calculate the excitation strengths $Z_j(p)$ relative to the density operator and hence the dynamic structure factor $S(p, \omega)$ [3]. Here, p and $\hbar\omega$ are the momentum and the energy transferred by a weak external probe. Differently from the Bogoliubov energies $\hbar\omega_j$, the strengths $Z_j(p)$, and $S(p, \omega)$, are not periodic functions of p , putting in clear evidence the difference between *momentum* and *quasi-momentum*.

We will often compare our numerical results with the predictions of the so called tight binding approximation, which is reached when the intensity of the laser field generating the optical lattice is so high that only the overlap between the wavefunctions of nearest-neighbour condensates plays a role. In the tight binding limit, the lowest

Bloch and Bogoliubov bands take analytic forms that will be discussed explicitly.

In Sect.IV, we study the effect of the lattice on the quantum depletion of the condensate and comment on the validity of Gross-Pitaevskii and Bogoliubov theory. Depending on the parameters of the problem, we distinguish between different configurations which show 3D, 2D or 1D features.

Finally, in Sect.V we include the presence of an additional harmonic trapping. This is achieved by employing a local density approximation to treat the inhomogeneity of the density profile due to the harmonic confinement. Important applications concern the frequencies of collective oscillations.

II. COMPRESSIBILITY AND EFFECTIVE MASS

The aim of this section is to calculate the compressibility and the effective mass as a function of the average density of the gas and of the depth of the optical potential. Using these quantities, we will also calculate the velocity of sound.

We consider the following geometry: along the z direction the atoms feel the periodic potential created by two counterpropagating laser fields, while the system is uniform in the transverse direction. The important length, momentum and energy scales of the problem are: the lattice spacing $d = \pi/k_{\text{opt}}$ related to the wavevector k_{opt} of the laser field in the lattice direction, the Bragg momentum $q_B = \hbar k_{\text{opt}} = \hbar\pi/d$ which identifies the edge of the Brillouin zone and the recoil energy $E_R = \hbar^2\pi^2/2md^2$, corresponding to the energy gained by an atom at rest by absorbing a lattice photon.

The trapping potential generated by the optical field can be simply written in the form

$$V(z) = s E_R \sin^2\left(\frac{\pi z}{d}\right), \quad (7)$$

where s is a dimensionless parameter which denotes the lattice depth in units of the recoil energy E_R .

The parameter characterizing the role of interactions in the system is gn , defined as the two-body coupling constant $g = 4\pi\hbar^2 a/m$ times the 3D *average* density n . Here a is the s-wave scattering length which will be always assumed to be positive. Typical values of the ratio gn/E_R used in recent experiments [4-7] range from 0.02 to 1.

Since the density is uniform in the transverse direction, the transverse degrees of freedom decouple from the axial ones and the stationary Gross-Pitaevskii equation can be reduced to a 1D equation of the form

$$\left[-\frac{\hbar^2}{2m} \frac{\partial^2}{\partial z^2} + s E_R \sin^2\left(\frac{\pi z}{d}\right) + gnd|\varphi(z)|^2 \right] \varphi(z) = \mu\varphi(z), \quad (8)$$

where the order parameter φ is normalized according to $\int_{-d/2}^{d/2} |\varphi(z)|^2 dz = 1$.

In spite of its non-linearity, Eq.(8) permits solutions in the form of Bloch waves

$$\varphi_{jk}(z) = e^{ikz/\hbar} \tilde{\varphi}_{jk}(z), \quad (9)$$

where k is the quasimomentum, j is the band index and the function $\tilde{\varphi}_{jk}(z)$ is periodic with period d . Notice that Eq.(9) does not exhaust all the possible stationary solutions of the Gross-Pitaevskii equation [8]. The Gross-Pitaevskii equation (8), rewritten in terms of the functions $\tilde{\varphi}_{jk}(z)$, reads

$$\left[\frac{1}{2m} (-i\hbar\partial_z + k)^2 + s E_R \sin^2 \left(\frac{\pi z}{d} \right) + gnd |\tilde{\varphi}_{jk}(z)|^2 \right] \tilde{\varphi}_{jk}(z) = \mu_j(k) \tilde{\varphi}_{jk}(z). \quad (10)$$

From the solution of Eq.(10) one gets the functions $\tilde{\varphi}_{jk}(z)$ and the corresponding chemical potentials $\mu_j(k)$.

The energy per particle $\varepsilon_j(k)$ can be calculated using the expression

$$\varepsilon_j(k) = \int_{-d/2}^{d/2} \tilde{\varphi}_{jk}^*(z) \left[\frac{1}{2m} (-i\hbar\partial_z + k)^2 + s E_R \sin^2(z) + \frac{1}{2} gnd |\tilde{\varphi}_{jk}(z)|^2 \right] \tilde{\varphi}_{jk}(z) dz. \quad (11)$$

and differs from the chemical potential $\mu_j(k)$. In fact by multiplying Eq.(10) by $\tilde{\varphi}_{jk}^*$ and integrating, one finds the expression

$$\mu_j(k) = \int_{-d/2}^{d/2} \tilde{\varphi}_{jk}^*(z) \left[\frac{1}{2m} (-i\hbar\partial_z + k)^2 + s E_R \sin^2(z) + gnd |\tilde{\varphi}_{jk}(z)|^2 \right] \tilde{\varphi}_{jk}(z) dz. \quad (12)$$

for the chemical potential which coincides with Eq.(11) only in absence of the interaction term. In general, μ_j and ε_j are related to each other by Eq.(1).

The solution of Eq.(10) for $k = 0$ and $j = 1$ gives the ground state of the system. This state corresponds to a condensate at rest in the frame of the optical lattice. Instead the solutions of Eq.(10) with $k \neq 0$, describe states of the system where all the atoms, occupying the same single-particle wavefunction, move together with respect to the optical potential giving rise to the constant current (4). Experimentally such states can be created by turning on adiabatically the intensity of a lattice moving at fixed velocity [4]. In this way, it is possible to map higher Brillouin zones onto higher bands.

Results for the Bloch bands (11) are shown in Fig.1 for $s = 5$ and $gn/E_R = 0, 0.1$ and 0.5 . The effect of interactions for these parameter values can be hardly distinguished in the energy band structure. It can be made more evident by plotting the group velocity

$$v = \frac{\partial \varepsilon(k)}{\partial k} \quad (13)$$

as a function of the quasi-momentum. For $gn = 0.5E_R$ one finds a difference in the group velocity of about 30% with respect to the non interacting case. The quantity plotted in Fig.1(b) is accessible experimentally through Bloch oscillations experiments [9]. In this context, it is important to note that the Bloch states (9) with $k \neq 0$ can become energetically or dynamically unstable depending on the choice of the values for s and gn (See for example [10–14]). Note also that for values of $gn \geq s$ one encounters loops (“swallow tails”) in the band structure at the band edge of the lowest band [12,15] and, at even smaller values of gn , at the center of the first excited band [12]. For the values of gn we have considered, these swallow tails exist only for very small values of the lattice depth s .

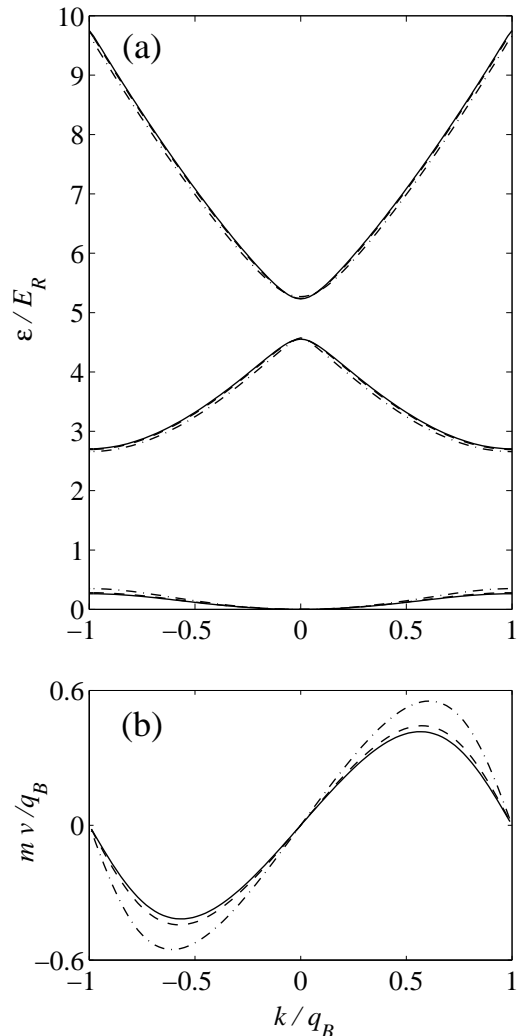


FIG. 1. (a) Lowest three Bloch bands for $s = 5$, $gn = 0$ (solid line), $0.1E_R$ (dashed line) and $0.5E_R$ (dash-dotted line). The energy of the groundstate ($k = 0$) has been subtracted; (b) Group velocity for the same parameters as in (a).

Let us now focus on the properties of the ground state ($k = 0, j = 1$). By solving numerically Eq.(10) and calculating the chemical potential, it is straightforward to evaluate the inverse compressibility (2) as a function of the relevant parameters of the problem. The results are plotted in Fig.2 as a function of gn for $s = 0, 5, 10$. The case $s = 0$ is the uniform case, where the equation of state is $\mu = gn$ and $\kappa^{-1} = gn$. In the presence of the optical lattice, we predict a deviation from this linear dependence on density. One finds an increase of the inverse compressibility with s , which is a direct consequence of the localization of the wavefunction at the bottom of the wells produced by the optical lattice. When the effect of two body interactions on the wavefunction is negligible one can account for this increase through the simple law $\kappa^{-1} = \tilde{g}(s)n$. The effective coupling constant $\tilde{g}(s)$ depends only on the lattice depth s and takes the explicit form

$$\tilde{g} = gd \int_{-d/2}^{d/2} \varphi_{gn=0}^4 dz, \quad (14)$$

where $\varphi_{gn=0}$ is the groundstate solution of Eq.(8) for $gn = 0$. It is correct to describe κ^{-1} with a linear dependence on the density only for small interaction parameters gn . For higher values of the interactions the slope of the curves tends to decrease. This is due to the fact that interactions tend to broaden the order parameter in each well and hence counteract the effect produced by the optical lattice. Numerical results for κ^{-1}/gn are presented in Fig.(3) and compared with the density independent quantity \tilde{g}/g (solid line), confirming that in general the compressibility does not depend linearly on the interaction. However for large s the density dependence of κ^{-1}/gn becomes less and less important and the expression $\kappa^{-1}(n, s) = \tilde{g}(s)n$ becomes applicable in a larger range of gn -values.

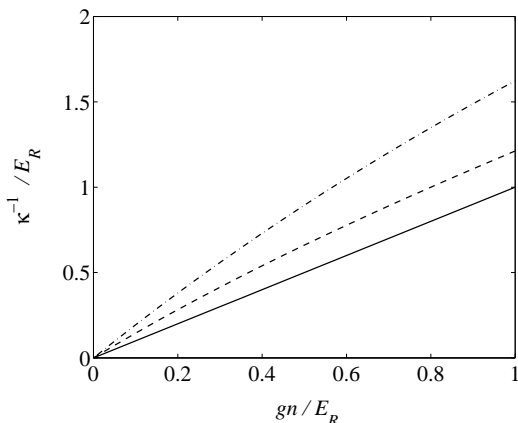


FIG. 2. Inverse compressibility $\kappa^{-1} = n\partial\mu/\partial n$ as a function of gn/E_R for $s = 0$ (solid line), $s = 5$ (dashed line) and $s = 10$ (dashed-dotted line).

Let us now determine the effective mass by studying the low- k behaviour of the lowest band $\varepsilon(k)$. The results

for $m^* = m^*(k = 0)$ are shown in Fig.4. For $s \rightarrow 0$, the effective mass tends to the bare mass m . Instead for large s the effective mass increases strongly due to the decreased tunneling between neighbouring wells of the optical potential. The effect of the interactions is to decrease the value of m^* as a consequence of the broadening of the wavefunction caused by the repulsion, which favours tunneling, contrasting the effect of the lattice potential. In fact, the effective mass is fixed by the tunneling properties of the system, which are exponentially sensible to the behaviour of the wavefunction in the region of the barriers. Then, any small change in the wavefunction due to interactions can have a significant effect on the effective mass.

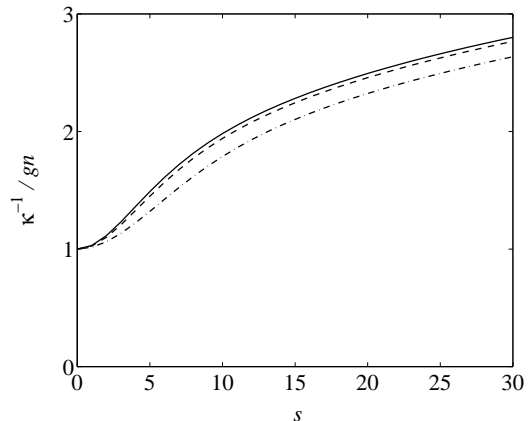


FIG. 3. κ^{-1}/gn for $gn = 0.1E_R$ (dashed line) and $gn = 0.5E_R$ (dashed-dotted line) as a function of the lattice depth s ; comparison with the effective coupling constant \tilde{g}/g defined in Eq.(14) (solid line).

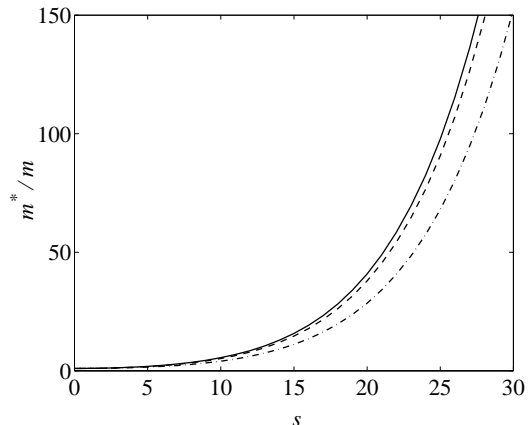


FIG. 4. Effective mass as a function of lattice depth s for $gn = 0$ (solid line), $gn = 0.1E_R$ (dashed line) and $gn = 0.5E_R$ (dashed-dotted line).

The two quantities calculated above, compressibility and effective mass, can be used to calculate the sound velocity using relation (6) [12,17]. The corresponding results are shown in Fig.5. We find that the sound velocity

decreases as the lattice is made deeper. This is due to the fact that the increase of the effective mass is more important than the decrease of the compressibility κ . The solid line in Fig.5 shows that decreasing the interactions the sound velocity approaches the law $c = \sqrt{\tilde{g}n/m_{gn=0}^*}$, where $m_{gn=0}^*$ is the effective mass calculated with $gn = 0$. The sound velocity is in principle measurable by studying the velocity of a wavepacket propagating in the presence of the optical potential. This could be done for example by following the experimental procedure used in [18]. Yet note that in deep lattices, non linear effects are expected to be important also for small amplitude perturbations [11].

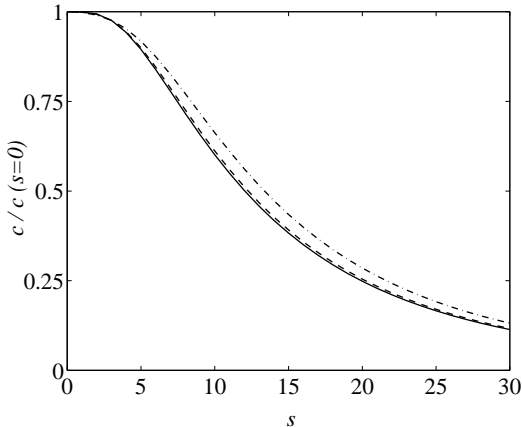


FIG. 5. Sound velocity as a function of the potential depth s divided by the sound velocity in the absence of the optical potential ($s = 0$) for $gn = 0.02E_R$ (solid line), $gn = 0.1E_R$ (dashed line) and $gn = 0.5E_R$ (dashed-dotted line).

Most of the results discussed above can be qualitatively understood by working in the so called tight binding approximation which becomes more and more accurate as the intensity of the laser field increases. Within the tight binding approximation we can derive analytic or semi-analytic expressions for the energy bands and consequently for the effective mass, compressibility and sound velocity.

Using Bloch's theorem, we can write the condensate in the lowest band as

$$\varphi_k(z) = \sum_l e^{ikld/\hbar} f(z - ld), \quad (15)$$

where l is the index of the well and f are the Wannier functions. The function $f(z)$ is normalised to unity and is orthogonal to the functions centered at different sites. In general, it depends on two-body interactions and hence on the density. Equation (15) holds for any depth of the optical potential. However, in the tight binding regime, $f(z)$ is a well localized function. This provides important simplifications in the calculation of the relevant quantities, since only nearest-neighbour overlap integrals have to be considered.

In our derivation of the tight binding results we will include also the interaction terms in the Hamiltonian. By substituting Eq.(15) into (10) and using definition (11) it follows, after some straightforward algebra, that the energy per particle takes the simple tight-binding form

$$\varepsilon(k) = \varepsilon - \delta \cos\left(\frac{kd}{\hbar}\right), \quad (16)$$

where $\varepsilon = \int f(z) \left[-\frac{\hbar^2 \partial_z^2}{2m} + V(z) + \frac{gnd}{2} f^2(z) \right] f(z) dz$ is an energy offset, which depends on s and gn but not on k , and δ is the tunneling parameter defined as

$$\delta = -2 \int f(z) \left[-\frac{\hbar^2 \partial_z^2}{2m} + V(z) + 2gnd f^2(z) \right] f(z-d) dz. \quad (17)$$

Using the same approximations, the chemical potential takes the form

$$\mu(k) = \mu_0 - \delta_\mu \cos\left(\frac{kd}{\hbar}\right), \quad (18)$$

where $\mu_0 = \int f(z) \left[-\frac{\hbar^2 \partial_z^2}{2m} + V(z) + gnd f^2(z) \right] f(z) dz$ and $\delta_\mu = \delta - 4gnd \int f^3(z) f(z-d) dz$. To derive Eqs.(16,18), we have kept terms of the order $\int f^3(z) f(z-d) dz$ and neglected terms of the order $\int f^2(z) f^2(z-d) dz$, which, for localized functions, turn out to be much smaller.

Note that δ and δ_μ depend on density both explicitly and implicitly through the density dependence of f (see Eq.(17)). In all situations considered in this work, contributions involving $\partial f / \partial n$ can be safely neglected. This approximation allows us to identify the quantity $\delta_\mu - \delta = -4gnd \int f^3(z) f(z-d)$ with $n \partial \delta / \partial n$.

To check the accuracy of the tight binding approximation, one can compare the numerical results for the first Bloch band with expression (16). The parameter δ is related to the curvature of the band at $k = 0$, i.e. to the effective mass defined in Eq.(3), through the important relation [19]

$$\delta = \frac{2}{\pi^2} \frac{m}{m^*} E_R. \quad (19)$$

Hence, we can evaluate (16) by using the numerical results for the effective mass discussed above (see Fig.(4)). In this way, we automatically include the correct density dependence of the tunneling parameter δ . In Fig.6, we compare the first Bloch energy band with its tight binding approximation for $gn = 0.5E_R$ and various values of s . The comparison shows that, for this value of the interactions, the tight binding approximation is already quite good for $s = 10$ and becomes better and better for increasing s .

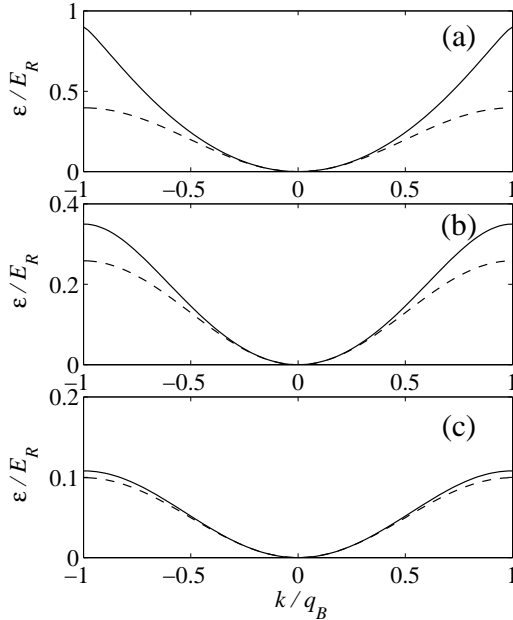


FIG. 6. Lowest Bloch band at $gn = 0.5E_R$ for different values of the potential depths: $s = 1$ (a), $s = 5$ (b) and $s = 10$ (c). The solid lines are obtained by evaluating Eq.(11) using the numerical solution of Eq.(10) while the dashed lines refer to the tight binding expression (16). The energy of the groundstate ($k = 0$) has been subtracted.

Using Eq.(18) for $k = 0$, we can also derive an expression for the inverse compressibility, which reads

$$\kappa^{-1} = gnd \int f^4(z)dz + 8gnd \int f^3(z)f(z-d)dz, \quad (20)$$

where contributions due to $\partial f/\partial n$ have been neglected, as previously. Since $\int f^3(z)f(z-d)dz$ is normally much smaller than $\int f^4(z)dz$, the on-site contribution to the inverse compressibility (first term in (20)) is usually the leading term.

A tight-binding expression for the density-independent effective coupling constant \tilde{g} (14) is obtained from (20) by replacing f with the Wannier function $f_{gn=0}$ of the non-interacting system. Then κ^{-1} is linear in the density and κ^{-1}/n can be identified with \tilde{g} . Neglecting the overlap contribution, \tilde{g} takes the form [17]

$$\tilde{g} = gd \int f_{gn=0}^4(z)dz. \quad (21)$$

This shows that in the tight binding regime, the effective coupling constant \tilde{g} can be safely estimated replacing the Bloch state $\varphi_{gn=0}$ in Eq.(14) by the Wannier function $f_{gn=0}$.

Deep in the tight binding regime, the function $f(z)$ can be conveniently approximated by a gaussian $f = \exp(-z^2/2\sigma^2)/\pi^{1/4}\sqrt{\sigma}$, where the width σ is chosen such as to satisfy the equation

$$-\frac{d^3}{\pi^3} \frac{1}{\sigma^3} + s \frac{\pi}{d} \sigma - s \frac{\pi^3}{d^3} \sigma^3 - \frac{1}{2} \frac{gn}{E_R} \sqrt{\frac{\pi}{2}} \frac{d^2}{\pi^2} \frac{1}{\sigma^2} = 0 \quad (22)$$

accounting for the anharmonicities of $\mathcal{O}(z^4)$ of the potential wells and for the broadening effect of repulsive two body interactions. Within the gaussian approximation, the inverse compressibility (20) can be rewritten in the simplified form

$$\kappa^{-1} = \frac{gnd}{\sqrt{2\pi}\sigma}, \quad (23)$$

where we have neglected the contribution arising from the overlap of neighbouring wavefunctions. If we neglect the interaction term in Eq. (22), we obtain $\kappa^{-1} = \tilde{g}n$, with $\tilde{g} = gd/\sqrt{2\pi}\sigma$ and $\sigma = s^{-1/4}(1 + 1/4\sqrt{s})d/\pi$. For $s = 10, gn = 0.5E_R$ the approximation (23) differs from the exact value of κ^{-1} by less than 1%.

Note that even though the gaussian approximation is useful in estimating the compressibility at high s , it can not be employed to calculate the effective mass or, equivalently, the tunneling parameter δ , which requires a more accurate description of the tails of the function f .

III. ELEMENTARY EXCITATIONS

In this section we study the spectrum of elementary excitations. We will focus our attention on the excitations relative to the ground state, i.e. to the solution of Eq.(10) with $j = 1$ (lowest band) and $k = 0$. To this aim we look for solutions of the time-dependent Gross-Pitaevskii equation of the form

$$\varphi(z, t) = e^{-i\mu t/\hbar} \left[\varphi(z) + u_{jq}(z)e^{-i\omega_j(q)t} + v_{jq}^*(z)e^{i\omega_j(q)t} \right], \quad (24)$$

where u_{jq} and v_{jq} describe a small perturbation with respect to the groundstate condensate $\varphi \equiv \varphi_{j=1, k=0}$. At first order in the perturbations, the time-dependent Gross-Pitaevskii equation yields the Bogoliubov equations

$$\left[-\frac{\hbar^2 \partial_z^2}{2m} + s E_R \sin^2\left(\frac{\pi z}{d}\right) - \mu + 2gnd|\varphi|^2 \right] u_{jq}(z) + gnd\varphi^2 v_{jq}(z) = \hbar\omega_j(q)u_{jq}(z), \quad (25)$$

$$\left[-\frac{\hbar^2 \partial_z^2}{2m} + s E_R \sin^2\left(\frac{\pi z}{d}\right) - \mu + 2gnd|\varphi|^2 \right] v_{jq}(z) + gnd\varphi^{*2}u_{jq}(z) = -\hbar\omega_j(q)v_{jq}(z). \quad (26)$$

The solutions u_{jq} and v_{jq} are Bloch waves ($u_{jq} = \exp(iz/\hbar)\tilde{u}_{jq}(z)$ where \tilde{u}_{jq} is periodic with period d and analogously for v_{jq}). They are labeled by their band index j and their quasimomentum q belonging to the first Brillouin zone. Hence, also the Bogoliubov spectrum $\omega_j(q)$ exhibits a band structure [20,21].

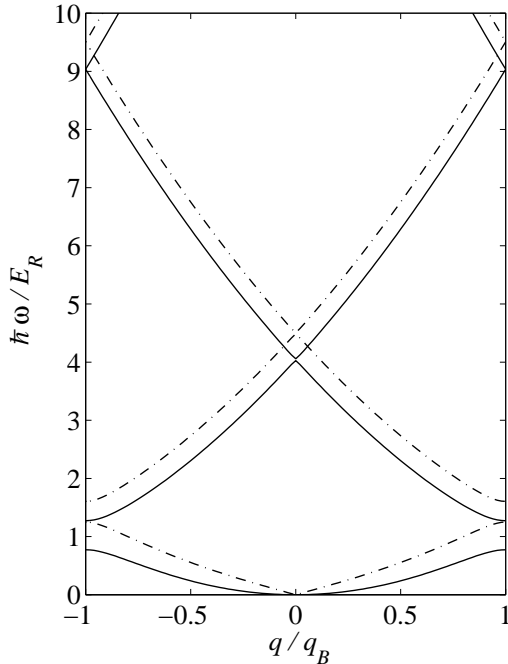


FIG. 7. Bogoliubov bands in the first Brillouin zone for $s = 1$, $gn = 0$ (solid line) and $gn = 0.5E_R$ (dash-dotted line). Note that for such a small potential, the gap between second and third band is still very small.

Similarities and differences with respect to the well-known Bogoliubov spectrum in the uniform case ($s = 0$) are immediate. As in the uniform case, interactions make the compressibility finite, giving rise to a phononic regime for long wavelength excitations ($q \rightarrow 0$) in the lowest band. In high bands the spectrum of excitations instead resembles the Bloch dispersion (see Eq.(11)). The differences are due to the fact that in the presence of the optical lattice the Bogoliubov spectrum develops a band structure. As a consequence, the dispersion is periodic as a function of quasimomentum and different bands are separated by an energy gap. In particular, the phononic regime present at $q = 0$ is repeated at every even multiple of the Bragg momentum q_B . Moreover, the lattice period d emerges as an additional physical length scale.

In Fig.7 we compare the Bogoliubov bands at $s = 1$ for $gn = 0$ and $gn = 0.5E_R$. In the interacting case, one notices the appearance of the phononic regime in the lowest band, while higher bands differ from the non-interacting ones mainly by an energy shift.

In Fig.8 we compare the lowest Bogoliubov and Bloch bands. Clearly, the lowest Bloch band is less affected by the presence of interactions than the Bogoliubov band. Recall that the Bogoliubov band gives the energy of the elementary excitations while the Bloch band gives the energy per particle of an excitation involving the whole condensate.

The solid lines in Fig.9 show how the lowest Bogoliubov band changes when the lattice depth is increased at fixed interaction. At $s = 1$ (Fig.9a), apart from the formation of the energy gap close to $q = q_B$, the curve still resembles

the dispersion in the uniform case: both the phononic linear regime and the quadratic regime are visible. When the potential is made deeper ($s = 5, 10$; Fig.9b,c), the band becomes flatter. As a consequence, the quadratic regime disappears and the slope of the phononic regime decreases. This reflects the behaviour of the velocity of sound (see Fig.5).

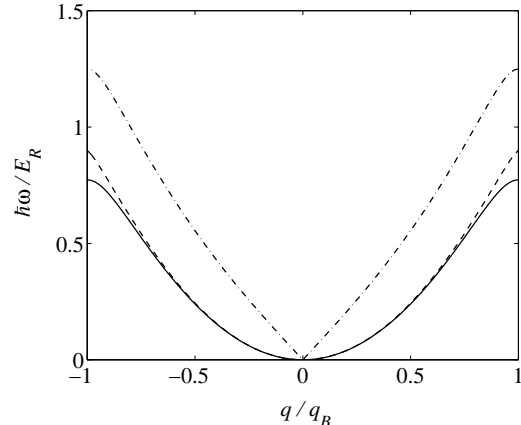


FIG. 8. Lowest Bloch band (dashed line) and lowest Bogoliubov band (dash-dotted line) bands for $s = 1$ and $gn = 0.5E_R$ compared with the energy band without interactions for $s = 1$ (solid line). The groundstate energy has been subtracted in the case of the Bloch band (dashed line) and of the energy band without interactions (solid line).

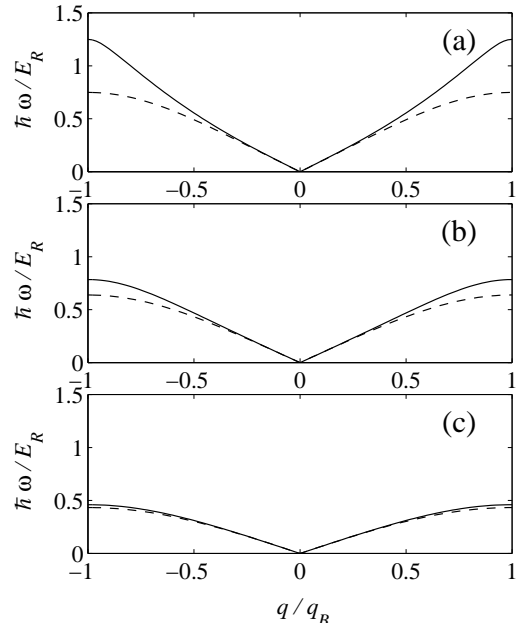


FIG. 9. Lowest Bogoliubov band at $gn = 0.5E_R$ for different values of the potential depths: $s = 1$ (a), $s = 5$ (b) and $s = 10$ (c). The solid lines are obtained from the numerical solution of Eqs.(25,26) while the dashed lines refer to the tight-binding expression (29).

Similarly to the Bloch energy and chemical potential spectra, also for the Bogoliubov excitation spectrum we can obtain an analytic expression in the tight binding limit. We write the excitation amplitudes in the form

$$u_q(z) = U_q \sum_l e^{iqld/\hbar} f(z - ld), \quad (27)$$

$$v_q(z) = V_q \sum_l e^{iqld/\hbar} f(z - ld), \quad (28)$$

where f is the same function as in (15). Recall, that $\int dz f^2 = 1$. Using expression (15) for the order parameter, we find the result

$$\hbar\omega_q = \sqrt{2\delta \sin^2\left(\frac{qd}{2\hbar}\right) \left[2\left(\delta + 2n\frac{\partial\delta}{\partial n}\right) \sin^2\left(\frac{qd}{2\hbar}\right) + 2\kappa^{-1} \right]} \quad (29)$$

for the excitation frequencies (lowest band), where δ and κ^{-1} are the tunneling and inverse compressibility parameters defined respectively in (17) and (20). In the same limit, the Bogoliubov amplitudes are

$$U_q = \frac{\varepsilon_q + \hbar\omega_q}{2\sqrt{\hbar\omega_q\varepsilon_q}}, \quad (30)$$

$$V_q = \frac{\varepsilon_q - \hbar\omega_q}{2\sqrt{\hbar\omega_q\varepsilon_q}}, \quad (31)$$

where ω_q is given by Eq.(29) and $\varepsilon_q = 2\delta \sin^2(qd/2\hbar)$ captures the quasimomentum dependence of the Bloch energy (compare with Eq.(16)). Note that in deriving Eqs.(30,31), we have imposed the normalization condition $\int_{-d/2}^{d/2} |u_q(z)|^2 - |v_q(z)|^2 dz = 1$.

In expression (29) the density dependence of the spectrum shows up in three different ways:

- first of all, the parameter δ depends on interactions as shown explicitly in Fig.4, where the quantity $m^* \propto 1/\delta$ (see relation (19)) is plotted;

- second, κ^{-1} has a more general dependence on the density than the one accounted for by the linear law $\tilde{g}n$, as shown in Fig.3;

- third, a contribution due to the density derivative of δ appears. However this term is always small: for small interactions one has $n\partial\delta/\partial n \ll \delta$ while for larger interactions the inverse compressibility κ^{-1} dominates both δ and $n\partial\delta/\partial n$. However, as shown in [13,14] this term can significantly affect the excitation frequency calculated on top of a moving condensate.

Fig.9 compares the numerical data with the approximate expression (29) evaluated using the parameters κ^{-1} and δ calculated in the previous section. The tunneling parameter δ is obtained from the data for the effective mass m^* through Eq.(19). As already found for the lowest Bloch band, for this value of gn , the agreement with the tight binding expression is already good for $s = 10$.

It is possible to identify two regimes, where the Bogoliubov spectrum can be described by further simplified expressions:

(I) for very large potential depth, the spectrum is dominated by the second term in the square brackets of Eq.(29). In fact, $\delta \rightarrow 0$ while κ^{-1} becomes larger and larger as s increases. Hence, the spectrum takes the form

$$\hbar\omega_q \approx \sqrt{\delta\kappa^{-1}} \left| \sin\left(\frac{qd}{2\hbar}\right) \right|, \quad (32)$$

both for large and small gn . Of course for large gn , the proper density-dependence of δ and κ^{-1} has to be taken into account in evaluating (32). Note that the Bogoliubov band becomes very flat since δ decreases exponentially for large lattice depth s . Yet, its height decreases more slowly than the lowest Bloch band (16) whose height decreases linearly in δ . We also point out that in the regime where Eq.(32) is valid, the Bogoliubov amplitudes Eqs.(30,31) become comparable in magnitude for all q in the first Brillouin zone, even if the excitation spectrum(32) is not linear. This implies that all excitations in the lowest band acquire quasi-particle character and the role of interactions is strongly enhanced.

(II) for small enough gn , one can neglect the density dependence of δ and use the approximation $\kappa^{-1} = \tilde{g}n$, where \tilde{g} was defined in (14) and takes the form (21) in the tight binding regime. This yields

$$\hbar\omega_q \approx \sqrt{2\delta_0 \sin^2\left(\frac{qd}{2\hbar}\right) \left[2\delta_0 \sin^2\left(\frac{qd}{2\hbar}\right) + 2\tilde{g}n \right]}, \quad (33)$$

which was first obtained in [22] (see also [11,23,24]). Eq.(33) has a form similar to the well-known Bogoliubov spectrum of uniform gases, the energy $2\delta_0 \sin^2(qd/2\hbar)$ replacing the free particle energy $q^2/2m$.

The spectrum of elementary excitations can be measured by exposing the system to a weak perturbation transferring momentum p and energy $\hbar\omega$. The response of the system is described by the dynamic structure factor $S(p, \omega)$ which, in the presence of a periodic potential takes the form

$$S(p, \omega) = \sum_j Z_j(p) \delta(\omega - \omega_j(p)), \quad (34)$$

where $Z_j(p)$ are the density excitation strengths relative to the j^{th} band and $\hbar\omega_j(p)$ are the corresponding excitation energies, defined by the solutions of Eqs.(25,26). Note that p , here assumed to be along the optical lattice (z axis), is not restricted to the first Brillouin zone, being the physical momentum transferred to the system by the external probe. In this respect, it is important to notice that, while the excitation energies $\hbar\omega_j(p)$ are periodic as a function of p , this is not true for the strengths $Z_j(p)$. Starting from the solution of Eqs.(25) and (26), the excitation strengths $Z_j(p)$ can be evaluated using the

standard prescription of Bogoliubov theory (see for example [25])

$$Z_j(p) = \left| \int_{-d/2}^{d/2} [u_{jq}^*(z) + v_{jq}^*(z)] e^{ipz/\hbar} \varphi(z) dz \right|^2, \quad (35)$$

where q belongs to the first Brillouin zone and is fixed by the relation $q = p + 2\ell q_B$ with ℓ integer and the Bogoliubov amplitudes are normalized according to $\int_{-d/2}^{d/2} |u_{jq}(z)|^2 - |v_{jq}(z)|^2 dz = 1$. The dynamic structure factor of a Bogoliubov gas in an optical lattice has been recently calculated in [3]. It is found that for an interacting system the strength towards the first band develops an oscillating behaviour as a function of the momentum transfer, vanishing at even multiples of the Bragg momentum due to the presence of a phononic regime. Moreover, in the presence of interactions, the strength Z_1 towards the first bands vanishes as $\sqrt{\delta\kappa}$ in the limit of very deep lattices, due to the quasi-particle character of the excitations in the whole band. Finally, the suppression of the static structure factor at small momenta, due to phononic correlations, is significantly enhanced by the presence of the lattice.

A. Link with the Josephson formalism

In this section, we show that the results for the excitation spectrum in the tight binding limit obtained in the previous section (see Eq.(29)) can be recovered using a different formalism based on the Josephson equations of motion. These can be derived starting from the ansatz for the condensate

$$\varphi(z, t) = \sum_l f_l(z; n_l) \sqrt{\frac{n_l(t)}{n}} e^{iS_l(t)}, \quad (36)$$

where for sufficiently deep optical lattices the wavefunction f_l is localized at site l and extends only over nearest-neighbouring sites, n_l is the time-dependent average density at site l where the average is taken over the l -th well, n is the average equilibrium density and S_l is the phase of the condensate at site l . At equilibrium the functions f_l coincide with the Wannier functions $f(z - ld)$ introduced before. In general, they depend on the density at the corresponding site, as indicated in Eq. (36), and hence might themselves implicitly depend on time. Furthermore, these functions are chosen such that $\int f_l^*(z; n_{l'}) f_l(z; n_l) dz = 0$ for $l \neq l'$ and 1 for $l = l'$.

When excitations are present, the phases S_l at different sites will be different from each other, indicating the presence of a current. Using the time-dependent Gross-Pitaevskii formalism one can derive the following equations of motion for the density and phase variables

$$\dot{n}_l = \sum_{l'=l+1, l-1} \frac{\delta^{l,l'}}{\hbar} \sqrt{n_l n_{l'}} \sin(S_l - S_{l'}), \quad (37)$$

$$\dot{S}_l = -\frac{\mu_l}{\hbar} + \sum_{l'=l+1, l-1} \frac{\delta_\mu^{l,l'}}{2\hbar} \sqrt{\frac{n_{l'}}{n_l}} \cos(S_l - S_{l'}), \quad (38)$$

where $\mu_l = \int f_l \left[-\frac{\hbar^2 \partial_z^2}{2m} + V(z) + gnd|f_l|^2 \right] f_l dz$, while the time-dependent tunneling parameters $\delta^{l,l'}$ and $\delta_\mu^{l,l'}$ are directly related to the overlap between two neighbouring wavefunctions

$$\delta^{l,l'} = -2 \int dz \left[f_l \left(-\frac{\hbar^2 \partial_z^2}{2m} + V \right) f_{l'} + gnd f_l |f_l|^2 f_{l'} + gn_{l'} d f_l |f_{l'}|^2 f_{l'} \right], \quad (39)$$

$$\delta_\mu^{l,l'} = \delta^{l,l'} - 4gnd \int f_l |f_l|^2 f_{l'} dz. \quad (40)$$

Note that at equilibrium $\delta^{l,l'} = \delta$ and $\delta_\mu^{l,l'} = \delta_\mu$, where δ and δ_μ have been previously defined in Eq.(17) and after Eq.(18). At equilibrium they do not depend on the sites l and l' since the wavefunctions f_l are all the same.

In order to obtain the excitation frequencies, one has to linearize Eqs.(37,38) around equilibrium: in Eq.(37) it is enough to take the value of $\delta^{l,l'}$ at equilibrium; instead in Eq.(38) one has to expand $\delta_\mu^{l,l'}$ to first order in the density fluctuations Δn_l

$$\delta_\mu^{l,l'} \approx \delta_\mu + \frac{\partial \delta_\mu^{l,l'}}{\partial n_l} \Delta n_l + \frac{\partial \delta_\mu^{l,l'}}{\partial n_{l'}} \Delta n_{l'}. \quad (41)$$

This procedure allows us to recover exactly Eq.(29). Instead, if one sets $\sqrt{n_l n_{l'}} = n_l$ from the beginning one obtains result (32) for the excitation spectrum. This proves that the first term in the brackets of Eq.(29) has its physical origin in the quantum pressure, because it arises from the difference in population $n_l - n_{l'}$ between neighbouring sites.

Note that in the form (37,38), the equations of motion differ from commonly used Josephson equations in that the quantities $\delta^{l,l'}$ and $\delta_\mu^{l,l'}$ can be time-dependent. In the usual treatment, these quantities are calculated at equilibrium and one approximates $\delta = \delta_\mu$. The resulting simplified equations are equivalent to the discrete nonlinear Schrödinger equation used for example in [26] to investigate nonlinear phenomena like solitons and breathers. An approach equivalent to the Josephson formalism presented in this section, based on the ansatz (36), has been developed independently in [13], where the approximations involved are discussed in detail.

For a system confined in the radial direction, containing N atoms per site, it is also convenient to introduce the Josephson energy $E_J = N\delta$ and the charging energy $E_C = 2\partial\mu/\partial N = 2\kappa^{-1}/N$ which play an important role in the physics of Josephson oscillations.

IV. QUANTUM FLUCTUATIONS AND DEPLETION OF THE CONDENSATE

The presence of the optical potential may introduce phase fluctuations which reduce the degree of coherence of the sample. This effect is known to yield spectacular consequences in 3D optical lattices, giving rise to a transition from the superfluid to the Mott insulator phases. Also in the presence of a 1D optical lattice one can predict interesting effects. First of all, the quantum depletion of the condensate increases as a consequence of the increase of the effective coupling constant (14) and of the effective mass. Eventually, if the tunneling rate becomes very small, the system reduces to a 1D chain of Josephson junctions with a modification of the behaviour of long range order affecting the phase coherence of the system.

Let us consider the problem in a 3D box, with the optical lattice oriented along the z -direction (Note that the quantum depletion of the condensate has been calculated in [23,24] for different geometries). The quantum numbers of the elementary excitations are the band index j and the quasi-momentum q along the z direction and the momenta p_x and p_y in the transverse directions. The quantum depletion of the condensate can be calculated using the Bogoliubov result

$$\frac{\Delta N_{\text{tot}}}{N_{\text{tot}}} = \frac{1}{N_{\text{tot}}} \sum_j \sum_{q, p_x, p_y} \int_{-d/2}^{d/2} dz \int dx \int dy |v_{j, q, p_x, p_y}(\mathbf{r})|^2, \quad (42)$$

where N_{tot} denotes the total number of atoms, ΔN_{tot} is the number of non-condensed particles and we sum over all bands j , over the quasi-momenta q in the first Brillouin zone and the momenta of elementary excitations in the transverse directions p_x, p_y allowed by the periodic boundary conditions. Eq. (42) describes correctly the depletion when Bogoliubov theory is applicable.

In the thermodynamic limit, the depletion can be calculated replacing the sum with an integral in Eq.(42). In the uniform case, the main contribution to the depletion is given by quasi-particles with $q^2 + p_x^2 + p_y^2 \approx (mc)^2$. Yet the convergence is very slow and the integral is saturated by momenta much higher than mc [27], where the dispersion exhibits the quadratic $p^2/2m$ behaviour. This implies that in the presence of the lattice it is possible to calculate the depletion as in the uniform case, provided all the quasimomenta relevant for the calculation of the depletion lie within the first Brillouin zone. This zone should include a region beyond the phononic regime where the dispersion goes like $q^2/2m^*$. This condition is satisfied if the inequality $m^*c \ll \kappa_B$ (or equivalently $\kappa^{-1} \ll \delta$), corresponding to weak interactions and relatively low values of s , is fulfilled. Under this condition, we can replace $q^2/2m \rightarrow q^2/2m^*$ and $g \rightarrow \tilde{g}$ and the quantum depletion takes the generalized Bogoliubov form

$$\frac{\Delta N_{\text{tot}}}{N_{\text{tot}}} = \frac{8}{3} \frac{1}{\pi^{1/2}} \sqrt{\frac{m^*}{m}} (\tilde{a}^3 n)^{1/2}, \quad (43)$$

where we have defined \tilde{a} through the relation $\tilde{g} = 4\pi\hbar^2\tilde{a}/m$. In this regime, the depletion will not be quantitatively very different from the corresponding one in the absence of the lattice. The situation becomes more interesting for larger optical potential depth, where the lattice is expected to affect the coherence properties of the system.

In the regime of deep optical lattices, one can neglect contributions to the depletion from higher bands, because high energy excitations are particle-like. We are then allowed to restrict the sum in (42) to $j = 1$. In the tight binding limit, one can easily generalize expressions (27,28) for the Bogoliubov amplitudes in the lowest band to account for transverse excitations

$$u_{q, p_x, p_y}(\mathbf{r}) = \frac{e^{i(p_x x + p_y y)/\hbar}}{L} U_{q, p_x, p_y} \sum_l e^{iqld/\hbar} f(z - ld), \quad (44)$$

$$v_{q, p_x, p_y}(\mathbf{r}) = \frac{e^{i(p_x x + p_y y)/\hbar}}{L} V_{q, p_x, p_y} \sum_l e^{iqld/\hbar} f(z - ld), \quad (45)$$

where $f(z)$ is the same function as in (15) and L is the transverse size of the system. Neglecting for simplicity contributions arising from $n\partial\delta/\partial n$, Eq.(29) can be generalized in a straightforward way to

$$\hbar\omega_q \approx \sqrt{\varepsilon_0(p_{\perp}, q)(\varepsilon_0(p_{\perp}, q) + 2\kappa^{-1})}, \quad (46)$$

where $\varepsilon_0(p_{\perp}, q) = p_{\perp}^2/2m + 2\delta \sin^2(qd/2\hbar)$ and $p_{\perp}^2 = p_x^2 + p_y^2$. For the amplitudes U_{q, p_x, p_y} and V_{q, p_x, p_y} we find the result

$$U_{q, p_x, p_y}, V_{q, p_x, p_y} = \frac{\varepsilon_0 \pm \hbar\omega}{2\sqrt{\hbar\omega\varepsilon_0}}, \quad (47)$$

satisfying the normalization condition $\int_{-d/2}^{d/2} dz \int dx \int dy [|u_{q, p_x, p_y}|^2 - |v_{q, p_x, p_y}|^2] = 1$.

We replace again the sum (42) by an integral. This corresponds to considering the thermodynamic limit in all the 3 directions. Inserting Eqs.(45,47), the calculation can be performed analytically and gives

$$\frac{\Delta N_{\text{tot}}}{N_{\text{tot}}} = 2 \frac{\tilde{a}}{d} G\left(\frac{\delta}{\tilde{g}n}\right), \quad (48)$$

where $G(b) = 1/2 - \sqrt{b}/\pi + b/2 - \arctan(\sqrt{b})(1+b)/\pi$ and, for simplicity we have used the approximation $\kappa^{-1} = \tilde{g}n$ for the compressibility. Since in the tight binding regime the ratio $\delta/\tilde{g}n$ is usually small and becomes smaller and smaller with increasing lattice depth, the result (48) converges to

$$\frac{\Delta N_{\text{tot}}}{N_{\text{tot}}} = \frac{\tilde{a}}{d}. \quad (49)$$

Result (49) coincides with the 2D depletion of a disc of axial extension d and scattering length \tilde{a} , where the axial confinement is so strong that the motion is frozen along the z -direction. In this limit the actual 3D system is

described as a series of separated 2D discs. It is interesting to note that the depletion remains finite even if the tunneling parameter $\delta \rightarrow 0$. The reason is that before taking the limit $\delta \rightarrow 0$ we have taken the continuum limit in the radial direction, which forces the system to be coherent. In this case the ratio $E_J/E_C = N\kappa\delta/2$ between the Josephson energy and the charging energy (see end of the last section) is large and hence coherence is maintained across the whole sample. A different result would be obtained by fixing N and considering the limit $\delta \rightarrow 0$. We point out that the dependence on the interaction strength is stronger in the 2D case than in the 3D case, since the depletion scales like \tilde{a} (2D) rather than $\tilde{a}^{3/2}$ (3D).

From Eq.(48), one recovers the 3D result (43) in the limit $\delta/\tilde{g}n \rightarrow \infty$. This limit is by the way only of academic interest, since in the tight binding limit, where (48) was derived, the ratio $\delta/\tilde{g}n$ becomes large only if interactions are vanishingly small (For example, for $gn = 0.02E_R$ and $s = 10$ one finds $\delta/\tilde{g}n \approx 1$).

Under the assumption made in the continuum approximation, the depletion is always very small and is upper-bounded by the quantity \tilde{a}/d . If the continuum approximation in the radial direction is not applicable and it is crucial to take into account the discretization of the sum over the quantum numbers p_x and p_y in Eq.(42), the results are different. This is the case if the number of particles in each well is sufficiently small, or if the longitudinal size of the system, fixed by the number of wells N_w , is sufficiently large. The limiting case takes place when the contribution arising from the term with $p_x = p_y = 0$ is the dominant one in Eq.(42). In this case the system exhibits typical 1D features and one finds the result

$$\frac{\Delta N_{\text{tot}}}{N_{\text{tot}}} = \nu \ln \left(\frac{4N_w}{\pi} \right), \quad (50)$$

where

$$\nu = \frac{m^*cd}{2\pi\hbar N}. \quad (51)$$

Here, N is the number of particles per well. The dependence on the interaction strength in the 1D case is stronger than in the 2D and 3D cases, since $c = \sqrt{\tilde{g}n/m^*}$ and hence the depletion scales like $\tilde{a}^{1/2}$. This should be compared with the \tilde{a} and $\tilde{a}^{3/2}$ dependence in 2D and 3D respectively.

The transition to the 1D character of the fluctuations can be identified by the condition

$$\frac{\tilde{a}}{d} \approx \nu \ln \left(\frac{4N_w}{\pi} \right), \quad (52)$$

which, for $gn = 0.2E_R$, $N_w = 200$ and $N = 500$, is predicted to occur around $s = 30$ where the left and right side of the inequality become equal to $\sim 4\%$.

Result (50,51) is strictly linked to the coherence theory of 1D systems, where the off-diagonal 1-body density exhibits the power law decay

$$n^{(1)}(|\mathbf{r} - \mathbf{r}'|) \rightarrow |\mathbf{r} - \mathbf{r}'|^{-\nu} \quad (53)$$

at large distances. If the exponent ν is much smaller than 1, the coherence survives at large distances and the application of Bogoliubov theory is justified. For a superfluid, the value of ν is fixed by the hydrodynamic fluctuations of the phase and is given, at $T = 0$, by the expression (51) [28,29]. In terms of the Josephson parameters (see section III A) one can also write $\nu = \sqrt{E_C/8\pi^2 E_J}$. One can easily check that, unless N is of the order of unity or m^* is extremely large, the value of ν always remains very small. When the exponent of the power law takes the value $\nu = 0.14$, corresponding to $E_J = 1.62E_C$, the 1D system is expected to exhibit the Bradley-Doniach phase transition to an insulating phase where the 1-body density matrix decays exponentially [30]. Note however that before this transition is reached the depletion (50) becomes large and hence Bogoliubov theory is no longer applicable.

To give an example, we set $gn = 0.2E_R$, $N = 200$ and $N_w = 500$ describing a setting similar to the experiment of [5]. Bogoliubov theory predicts a depletion of $\approx 0.6\%$ in the absence of the lattice ($s = 0$). At a lattice depth of $s = 10$ the evaluation of Eq.(42), using the tight binding results (45,47), and keeping the sum discrete yields a depletion of $\approx 1.7\%$. On the other hand, Eq.(48), obtained by replacing the sum in Eq.(42) by an integral, yields a depletion of $\approx 2\%$, in reasonable agreement with the full result $\approx 1.7\%$. The 2D formula (49) instead yields $\approx 2.9\%$ depletion, revealing that the system is not yet fully governed by 2D fluctuations. With the same choice of parameters, the power law exponent (51) has the value $\nu = 0.001$ and the 1D depletion (50) is predicted to be $\approx 0.6\%$, significantly smaller than the full value $\approx 1.7\%$. This reveals that the sum (42) is not exhausted by the terms with $p_x = p_y = 0$. In conclusion, one finds that for this particular setting, the character of fluctuations is intermediate between 3D and 2D, and still far from 1D. In particular, from the above estimates it emerges that in order to reach the conditions for observing the Bradley-Doniach transition one should work at much larger values of s .

V. APPLICATIONS TO HARMONICALLY TRAPPED CONDENSATES

The results obtained in the previous sections can be used to describe harmonically trapped condensates in the presence of an optical lattice: If the trapped condensate is well described by the TF-approximation in the absence of the lattice and if the axial size of the condensate is much larger than the interwell separation d , then one can generalize the local density approximation (LDA) to

describe harmonically trapped condensates in a lattice. Basically, the idea is to introduce the average density

$$n_l(r_\perp) = \frac{1}{d} \int_{ld-d/2}^{ld+d/2} n(r_\perp, z) dz, \quad (54)$$

where $n(r_\perp, z)$ is the microscopic density and l is the index of the lattice sites. Within the LDA, the chemical potential is given by

$$\mu_l = \mu_{\text{opt}}(n_l(r_\perp)) + \frac{m}{2}(\omega_z^2 l^2 d^2 + \omega_\perp^2 r_\perp^2), \quad (55)$$

where $\mu_{\text{opt}}(n_l(r_\perp))$ is the chemical potential calculated at the average density $n_l(r_\perp)$ in the presence of the optical potential and ω_z, ω_\perp are the axial and transverse frequencies of the harmonic trap respectively. Eq.(55) fixes the radial density profile $n_l(r_\perp)$ at the l -th site once the value of μ_l or, equivalently, the number of atoms

$$N_l = 2\pi d \int_0^{R_l} r_\perp dr_\perp n_l(r_\perp), \quad (56)$$

occupying the l -th well is known. In Eq.(56), R_l is the radial size of the condensate at the l -th site, fixed by the value of r_\perp where the density $n_l(r_\perp)$ vanishes. This procedure avoids the full calculation of the microscopic density $n(r_\perp, z)$.

When equilibrium is established across the whole sample we have $\mu_l = \mu$ for all l . Making use of this fact and employing that $\sum_l N_l = N_{\text{tot}}$ we can find the dependence of μ on the total number of particles N_{tot} . This procedure also yields the well occupation numbers N_l and the number of sites occupied at equilibrium. In the simple case in which the chemical potential exhibits a linear dependence on density $\mu_{\text{opt}} = \tilde{g}n + \text{const.}$ one obtains for the radial density profile [31]

$$n_l(r_\perp) = \frac{1}{\tilde{g}} \left(\mu - \frac{m}{2}\omega_z^2 l^2 d^2 - \frac{m}{2}\omega_\perp^2 r_\perp^2 \right), \quad (57)$$

where the chemical potential, apart from a constant, is given by $\mu = \hbar\tilde{\omega}(15N_{\text{tot}}a\tilde{g}/a_{\text{ho}}g)^{2/5}/2$ with $\tilde{\omega} = (\omega_x\omega_y\omega_z)^{1/3}$, $a_{\text{ho}} = \sqrt{\hbar/m\tilde{\omega}}$. The well occupation numbers and transverse radii are given by

$$N_l = N_0 (1 - l^2/l_m^2)^2, \quad (58)$$

$$R_l = R_0 (1 - l^2/l_m^2)^{1/2}, \quad (59)$$

where $l_m = \sqrt{2\mu/m\omega_z^2 d^2}$ fixes the number $2l_m + 1$ of occupied sites, $N_0 = 15N/16l_m$ and $R_0 = \sqrt{2\mu/m\omega_\perp^2}$. The increase of μ due to the optical lattice ($\tilde{g} > g$) implies an increase of the radii R_l . This effect has been observed in the experiment of [6].

The LDA-based approach not only permits to calculate equilibrium properties, but also dynamic features of macroscopic type. To this purpose one can generalize the hydrodynamic equations of superfluids by taking into account the effects of the lattice. Also in this case one can

use the concept of the average density profile $n_l(r_\perp)$ as defined in Eq.(54). Furthermore, one can replace the discrete index l by the continuous variable $z = ld$. In this way, one can define a smoothed macroscopic average density profile $n_M(r_\perp, z)$. The dynamics we are interested in then consists of the evolution of the macroscopic density n_M and of the macroscopic superfluid velocity field \mathbf{v} whose component along the direction of the lattice is defined by the average

$$\begin{aligned} v_z &= \frac{1}{D} \int_{-D/2}^{D/2} dz \left[\frac{\hbar}{m} \partial_z S \right] \\ &= \frac{\hbar}{m} \frac{1}{D} (S(D/2) - S(-D/2)). \end{aligned} \quad (60)$$

Here S is the phase of the order parameter and D is a length longer than d , but small compared to the size of the system as well as to the wavelength of the collective oscillations. On this length scale, the effect of V_{ho} can be neglected and all the macroscopic variables are constant. Hence the phase difference in (60) can be calculated using Bloch states with quasimomentum k (see Eq.(9)) and one finds the result $v_z = k/m$ [32]. Using this result and the fact that the energy change per particle due to the presence of a small current is $k^2/2m^* = m^2 v_z^2/2m^*$, the use of the LDA yields the result

$$\begin{aligned} E &= \int d\mathbf{r} \left[\frac{m}{2} n_M v_x^2 + \frac{m}{2} n_M v_y^2 + \frac{m}{2} \frac{m}{m^*} n_M v_z^2 \right. \\ &\quad \left. + e(n_M) + n_M V_{\text{ho}} \right], \end{aligned} \quad (61)$$

for the total energy of the system. Here $e(n_M)$ is the equilibrium energy per unit volume calculated at the average density n_M in the absence of the harmonic trap and both n_M and v_z are now functions of r_\perp, z and t .

Starting from the functional (61) we can derive the hydrodynamic equations

$$\frac{\partial}{\partial t} n_M + \partial_x (v_x n_M) + \partial_y (v_y n_M) + \partial_z \left(\frac{m}{m^*} v_z n_M \right) = 0 \quad (62)$$

$$\begin{aligned} m \frac{\partial}{\partial t} \mathbf{v} + \nabla (V_{\text{ho}} + \mu_{\text{opt}}(n_M)) \\ + \frac{m}{2} v_x^2 + \frac{m}{2} v_y^2 + \frac{\partial}{\partial n_M} \left(\left(\frac{m}{m^*} n_M \right) \frac{m}{2} v_z^2 \right) = 0, \end{aligned} \quad (63)$$

where $V_{\text{ho}} = m(\omega_z^2 z^2 + \omega_\perp^2 r_\perp^2)/2$ is the harmonic potential and where we have used the relationship $\mu_{\text{opt}} = \partial e(n_M)/\partial n_M$. Eqs.(62,63) generalize the hydrodynamic equations derived in [17] to situations in which the effective mass is density dependent and the chemical potential μ_{opt} has a nonlinear density dependence (see section (II)). They can be further generalized to account for larger condensate velocities [12].

The hydrodynamic equations serve to determine the frequencies of collective oscillations associated with a density dynamics of the form $n_M(\mathbf{r}, t) = \bar{n}_M(\mathbf{r}) + e^{-i\omega t} \delta n(\mathbf{r})$. Here, $\delta n(\mathbf{r})$ denotes a small deviation from the equilibrium average density $\bar{n}_M(\mathbf{r})$ that is associated

with a small velocity field \mathbf{v} . Hence, it is appropriate to linearize Eqs.(62,63) yielding

$$\omega^2 \delta n + \partial_{\mathbf{r}_\perp} \left[\frac{\bar{n}_M}{m} \partial_{\mathbf{r}_\perp} \left(\left. \frac{\partial \mu_{\text{opt}}}{\partial n} \right|_{\bar{n}_M} \delta n \right) \right] + \partial_z \left[\frac{\bar{n}_M}{m^*} \partial_z \left(\left. \frac{\partial \mu_{\text{opt}}}{\partial n} \right|_{\bar{n}_M} \delta n \right) \right] = 0. \quad (64)$$

This second order equation involves the derivative $\partial \mu_{\text{opt}} / \partial n|_{\bar{n}_M}$ directly related to the inverse compressibility κ^{-1} (see Eq.(2)). In general, the solution of Eq.(64) should be found numerically because the density dependence of m^* and $\partial \mu_{\text{opt}} / \partial n$ is not known in an analytic form. Yet, for small enough densities the density-dependence of m^* can be neglected and $\partial \mu_{\text{opt}} / \partial n|_{\bar{n}_M} = \tilde{g}$ as was discussed in Sect.(II). In this case, the frequencies of the collective oscillations can be calculated analytically [17]. In particular, they can be obtained from the values in the absence of the lattice [33] by simply rescaling the trapping frequency along z

$$\omega_z \rightarrow \sqrt{\frac{m}{m^*}} \omega_z. \quad (65)$$

This result was obtained theoretically for the dipole oscillation in the tight binding regime in [5] and has been confirmed experimentally both for the dipole [5] and quadrupole oscillation [34].

The LDA defined by (55) can also be employed to study Bogoliubov excitations occurring on a length scale much smaller than the size of the system. Under this condition, one can define a local Bogoliubov band spectrum given by $\hbar \omega_j(q; n_M(\mathbf{r}))$ where $n_M(\mathbf{r})$ is the locally averaged density introduced above. The Bogoliubov band spectrum can be probed by measuring the dynamic structure factor $S(p, \omega)$, related to the linear response of the system to an external perturbation transferring momentum p and energy $\hbar \omega$. In LDA, the dynamic structure factor reads [35]

$$S_{LDA}(p, \omega) = \int d\mathbf{r} n_M(\mathbf{r}) S(p, \omega; \mathbf{r}), \quad (66)$$

where $S(p, \omega; \mathbf{r})$ is the dynamic structure factor (34) calculated at density $n_M(\mathbf{r})$ in the absence of harmonic trapping. As a result of the averaging implied by Eq.(66), the dynamic structure factor of the system is not any more given by a series of delta-functions as in the absence of the harmonic trap, but instead consists of resonances of finite width. The validity of the LDA to describe the linear response of the trapped condensate in the absence of a lattice has been confirmed by Bragg spectroscopy experiments where the transferred momentum was larger than the inverse of the system size and the duration of the Bragg pulse was small compared to the inverse of the trapping frequencies [36,37]. Experiments and calculations which investigate the regime beyond the validity of the LDA have been recently carried out [37,38].

In the absence of harmonic trapping, the solution of the hydrodynamic equations (62) and (63) permits to calculate the propagation of sound waves not only in condensates at rest, yielding result (6) for the sound velocity, but also in condensates moving slowly with respect to the lattice. Let us start from stationary solution with macroscopic velocity \bar{v}_z , corresponding to quasimomentum $k = m\bar{v}_z$, with $k \ll q_B$, and let us consider small changes of the velocity field and of the density with respect to the stationary values: $v_z = \bar{v}_z + \delta v_z$, $n_M = \bar{n}_M + \delta n_M$. By linearizing Eqs.(62) and (63) and looking for solutions oscillating like $\sim e^{-i(qz - \omega t)}$, one finds at first order in k

$$\omega = c|q| + q \frac{k}{m_\mu^*}, \quad (67)$$

where $1/m_\mu^* = \partial(n/m^*)/\partial n$ and c is the sound velocity in the condensate at rest (see Eq.(6)). The quantity m_μ^* gives the $k = 0$ curvature of the lowest chemical potential band (see Eq.(12) with $j = 1$) according to $\mu(k) = \mu(0) + k^2/2m_\mu^*$ for $k \rightarrow 0$. Eq.(67) generalizes the usual behaviour of the sound velocity in slowly moving frames to account for the presence of the optical lattice. The significance of m_μ^* for the excitation spectrum has been pointed out for any optical potential depth for small q and any k in [12] and in the tight binding regime for any q and any k in [13,14].

VI. SUMMARY

We have studied Bloch-wave solutions of the Gross-Pitaevskii equation in the presence of a one-dimensional optical lattice. In particular, we have calculated the band structure of both stationary (“Bloch bands”) and time-dependent linearized (“Bogoliubov bands”) solutions. We have discussed these solutions for different choices of the lattice depth sE_R and the two body interaction parameter gn . Special attention has been paid to the behaviour of the compressibility and of the effective mass. We have shown that the compressibility of the system is reduced by the presence of the lattice and that its inverse is approximately linear in the density for low enough gn or high s . In these regimes, the compressibility and the chemical potential can be expressed in terms of an effective coupling constant $\tilde{g} > g$, which accounts for the squeezing of the condensate wavefunction in each well. Concerning the effective mass we have found that two body interactions give rise to a significant density dependence which decreases its value with respect to the prediction for the non-interacting system. The compressibility and the effective mass permit to calculate the sound velocity whose value is found to decrease as a function of the lattice depth, reflecting the exponential increase of the effective mass. For the tight binding regime, we have complemented the numerical results by analytic expressions.

Concerning the Bogoliubov bands, we have found that in a deep lattice the excitations in the lowest band acquire a strong quasi-particle character in the whole Brillouin zone, characterized by Bogoliubov amplitudes $u \sim v$. In the tight binding regime, analytic expressions for the lowest Bogoliubov band and the corresponding Bogoliubov amplitudes have also been reported.

In section IV, we have presented results for the quantum depletion of the condensate. In particular, we have found that in a deep lattice the quantum fluctuations of the condensate acquire 2D character, reflecting the transformation of the system into a series of two-dimensional discs. As a consequence, the quantum depletion increases, but remains small, provided the coherence between the discs is maintained. If the lattice depth is increased further, 1D quantum fluctuations become important. Estimates of the corresponding effects with realistic values of the parameters have been presented.

Finally, we have demonstrated the use of a local density approximation to study macroscopic static and dynamic properties of harmonically trapped systems in the presence of an optical lattice.

In conclusion, Bose-Einstein condensates in optical lattices share important analogies with solid state systems. Differences arise due to the presence of two body interactions giving rise to important new features even in the coherent regime where most particles are in the condensate. The density dependence of the effective mass, as well as the distinction between Bloch, chemical potential and Bogoliubov bands are some examples discussed in this paper. Natural developments of the present work concern the study of the dynamics built on top of moving condensates where dynamic instabilities can be encountered [10–14]. Another important direction is the study of nonlinear effects which might sizeably affect the propagation of sound in the presence of an optical lattice.

VII. ACKNOWLEDGMENTS

We would like to thank M.L. Chiofalo, O. Morsch and A. Smerzi for useful discussions. This research is supported by the Ministero dell’Istruzione, dell’Università e della Ricerca (MIUR).

[1] D. Jaksch, C. Bruder, J.I. Cirac, C.W. Gardiner and P. Zoller, Phys. Rev. Lett. **81**, 3108 (1998).
 [2] M. Greiner, O. Mandel, T. Esslinger, T.W. Hänsch and I. Bloch, Nature **415**, 39 (2002).
 [3] C. Menotti, M. Krämer, L. Pitaevskii and S. Stringari, Phys. Rev. A **67**, 053609 (2003).
 [4] J.H. Denschlag, J.E. Simsarian, H. Häffner, C. McKenzie, A. Browaeys, D. Cho, K. Helmerson, S.L. Rolston and W.D. Phillips, J. Phys. B **35**, 3095 (2002).

[5] F.S. Cataliotti, S. Burger, C. Fort, P. Maddaloni, F. Minardi, A. Trombettoni, A. Smerzi and M. Inguscio, Science **293**, 843 (2001).
 [6] O. Morsch, M. Cristiani, J.H. Müller, D. Ciampini, and E. Arimondo, Phys. Rev. A **66**, 021601 (2002).
 [7] M. Greiner, I. Bloch, O. Mandel, T.W. Hänsch, and T. Esslinger, Phys. Rev. Lett. **87**, 160405 (2001).
 [8] M. Machholm, A. Nicolin, C.J. Pethick, and H. Smith, cond-mat/0307183.
 [9] O. Morsch, J.H. Müller, M. Cristiani, D. Ciampini, and E. Arimondo, Phys. Rev. Lett. **87**, 140402 (2001). M. Cristiani, O. Morsch, J.H. Müller, D. Ciampini, and E. Arimondo, Phys. Rev. A **65**, 063612 (2002).
 [10] B. Wu, Q. Niu, Phys. Rev. A **64**, 061603 (2001).
 [11] A. Smerzi, A. Trombettoni, P.G. Kevrekidis, A.R. Bishop, Phys. Rev. Lett. **89**, 170402 (2002).
 [12] M. Machholm, C.J. Pethick, and H. Smith, Phys. Rev. A **67**, 053613 (2003).
 [13] A. Smerzi and A. Trombettoni, Chaos **13**, 766 (2003). A. Smerzi and A. Trombettoni, Phys. Rev. A **68**, 023613 (2003).
 [14] C. Menotti, A. Smerzi, and A. Trombettoni, New J. Phys. **5**, 112 (2003).
 [15] B. Wu and Q. Niu, Phys. Rev. A **61**, 023402 (2000). B. Wu, R.B. Diener, and Q. Niu, Phys. Rev. A **65**, 025601 (2002). D. Diakonov, L.M. Jensen, C.J. Pethick, and H. Smith, Phys. Rev. A **66**, 013604 (2002). E.J. Mueller, Phys. Rev. A **66**, 063603 (2002).
 [16] D.I. Choi and Q. Niu, Phys. Rev. Lett **82**, 2022 (1999).
 [17] M. Krämer, L. Pitaevskii and S. Stringari, Phys. Rev. Lett **88**, 180404 (2002).
 [18] M.R. Andrews, D.M. Kurn, H.-J. Miesner, D.S. Durfee, C.G. Townsend, S. Inouye, and W. Ketterle, Phys. Rev. Lett. **79**, 553 (1997).
 [19] Analogously, using Eq.(1), one finds the relation $\delta_\mu/E_R = 2m/m_\mu^* \pi^2$ where $1/m_\mu^* = \partial(n/m^*)/\partial n$ is the curvature of the band $\mu_{j=1}(k)$ at $k = 0$ and δ_μ has been defined in Eq.(18).
 [20] K. Berg-Sørensen and K. Mølmer, Phys. Rev. A **58**, 1480 (1998).
 [21] M.L. Chiofalo, M. Polini and M.P. Tosi, Eur. Phys. J. D **11**, 371 (2000).
 [22] J. Javanainen, Phys. Rev. A **60**, 4902 (1999).
 [23] D. van Oosten, P. van der Straten, and H. T. C. Stoof, Phys. Rev. A **63**, 053601 (2001).
 [24] A.M. Rey, K. Burnett, R. Roth, M. Edwards, C.J. Williams, and C.W. Clark, J. Phys. B **36**, 825 (2003).
 [25] W.-C. Wu and A. Griffin, Phys. Rev. A **54**, 4204 (1996).
 [26] A. Trombettoni and A. Smerzi, Phys. Rev. Lett. **86**, 2353 (2001).
 [27] F. Dalfovo, S. Giorgini, M. Guilleumas, L. Pitaevskii, and S. Stringari, Phys. Rev. A **56**, 3840 (1997).
 [28] L. Pitaevskii and S. Stringari, *Bose-Einstein Condensation* (Oxford University Press, Oxford, 2003).
 [29] The case without lattice is discussed in K.B. Efetov and A.I.Larkin, Sov. Phys. JETP **42**, 390 (1975). F.D.M. Haldane, Phys. Rev. Lett. **47**, 1840 (1981). V.N. Popov, JETP Lett. **31**, 526 (1980).
 [30] R.M. Bradley and S. Doniach, Phys. Rev. B **30**, 1138

- (1984).
- [31] P. Pedri, L. Pitaevskii, S. Stringari, C. Fort, S. Burger, F.S. Cataliotti, P. Maddaloni, F. Minardi, M. Inguscio, Phys. Rev. Lett. **87**, 220401 (2001). There, μ_l was defined in a different way: $\mu_l = \mu - m\omega_z^2 d^2 l^2 / 2$ at equilibrium.
 - [32] The superfluid velocity should not be confused with the group velocity (13), which, for $k \rightarrow 0$, approaches the value $\partial\varepsilon/\partial k = k/m^*$.
 - [33] S. Stringari, Phys. Rev. Lett. **77**, 2360 (1996).
 - [34] C. Fort, F.S. Cataliotti, L. Fallani, F. Ferlaino, P. Maddaloni, and M. Inguscio, Phys. Rev. Lett. **90**, 140405 (2003).
 - [35] F. Zambelli, L. Pitaevskii, D.M. Stamper-Kurn and S. Stringari, Phys. Rev. A **61**, 063608 (2000). A. Brunello, F. Dalfovo, L. Pitaevskii, S. Stringari, and F. Zambelli, Phys. Rev. A **64**, 063614 (2001).
 - [36] J. Stenger, S. Inouye, A.P. Chikkatur, D.M. Stamper-Kurn, D.E. Pritchard, and W. Ketterle, Phys. Rev. Lett. **82**, 4569 (1999). D.M. Stamper-Kurn, A.P. Chikkatur, A. Görlitz, S. Inouye, S. Gupta, D.E. Pritchard, and W. Ketterle, Phys. Rev. Lett. **83**, 2876 (1999). J.M. Vogels, K. Xu, C. Raman, J.R. Abo-Shaeer, and W. Ketterle, Phys. Rev. Lett. **88**, 060402 (2002). J. Steinhauer, R. Ozeri, N. Katz, and N. Davidson, Phys. Rev. Lett. **88**, 120407 (2002). R. Ozeri, J. Steinhauer, N. Katz, and N. Davidson, Phys. Rev. Lett. **88**, 220401 (2002).
 - [37] J. Steinhauer, N. Katz, R. Ozeri, N. Davidson, C. Tozzo, and F. Dalfovo, Phys. Rev. Lett. **90**, 060404 (2003).
 - [38] C. Tozzo and F. Dalfovo, New J. Phys. **5**, 54 (2003).